MICROBIAL ECOLOGY

Microb Ecol (2003) 46:200–215
DOI: 10.1007/s00248-002-0003-x

Structure and Seasonal Dynamics of Hyporheic Zone Microbial Communities in Free-Stone Rivers of the Western United States

K.P. Feris, P.W. Ramsey, C. Frazar, M.C. Rillig, J.E. Gannon, W.E. Holben

Microbial Ecology Program, Division of Biological Sciences, The University of Montana, Missoula MT 59812-1002 USA

Received: 22 October 2002; Accepted: 15 January 2003; Online publication: 13 June 2003

ABSTRACT

The hyporheic zone of a river is characterized by being nonphotic, exhibiting chemical/redox gradients, and having a heterotrophic food web based on the consumption of organic carbon entrained from surface waters. Hyporheic microbial communities constitute the base of food webs in these environments and are important for maintaining a functioning lotic ecosystem. While microbial communities of rivers dominated by fine-grained sediments are relatively well studied, little is known about the structure and seasonal dynamics of microbial communities inhabiting the predominantly gravel and cobble hyporheic zones of rivers of the western United States. Here, we present the first molecular analysis of hyporheic microbial communities of three different stream types (based on mean base discharge, substratum type, and drainage area), in Montana. Utilizing 16S rDNA phylogeny, DGGE pattern analysis, and qPCR, we have analyzed the prokaryotic communities living on the 1.7 to 2.36 mm grain-size fraction of hyporheic sediments from three separate riffles in each stream. DGGE analysis showed clear seasonal community patterns, indicated similar community composition between different riffles within a stream (95.6–96.6% similarity), and allowed differentiation between communities in different streams. Each river supported a unique complement of species; however, several phylogenetic groups were conserved between all three streams including Pseudomonads and members of the genera *Aquabacterium*, *Rhodoferax*, *Hyphomicrobium*, and *Pirellula*. Each group showed pronounced seasonal trends in abundance, with peaks during the Fall. The *Hyphomicrobium* group was numerically dominant throughout the year in all three streams. This work provides a framework for investigating the effects of various environmental factors and anthropogenic effects on microbial communities inhabiting the hyporheic zone.

Introduction

The hyporheic zone is the region of saturated sediments beneath the channel of a stream [43] and is an important component of lotic ecosystems [16, 56, 58]. This transition

Correspondence to: W.E. Holben; E-mail: bholben@selway.umt.edu

zone between surface and groundwater lends connectivity between these two environments [9, 68]. The hyporheic zone can simultaneously support seemingly contradictory metabolic types because of its heterogeneous nature and characteristic gradients of inorganic nutrients, Eh, and organic carbon [1, 6]. Because of the absence of light in this environment, the food web is based primarily on the consumption of organic carbon entrained from surface waters [1, 17, 50]. The microbial communities that reside in the hyporheic zone of lotic ecosystems play important roles in nutrient retention [47] and cycling, constitute the majority of the biomass and activity in these systems [11, 19, 20, 55], and can account for 76–96% of ecosystem respiration [48]. In some rivers with extensive alluvial aquifers, such as those found in western Montana, the productivity of the hyporheic zone can be orders of magnitude greater than that in benthic sediments [11].

Previous investigations into the structure of hyporheic communities have largely been based on measures of invertebrate distribution and abundance [1, 6, 21, 46, 51, 75] or on total bacterial biomass [7, 17, 20, 22, 57, 67]. The majority of information on the microbial component of the hyporheos (the biotic component of the hyporheic zone) is based on community-level physiological measures such as respiration [14] and productivity [7]. To date, only a few investigations have attempted to describe the structure and seasonal dynamics of hyporheic microbial communities [2, 67]. Smoot and Findlay [67] demonstrated seasonal variation in bacterial biomass and community structure, as measured by PLFA analysis, for microbial communities associated with riverine and lacustrine sediments in a hybrid river-lake ecosystem. Battin et al. [2] identified the β-proteobacteria subclass as the dominant component of lotic biofilms and provided the first evidence of Archaea in a lotic ecosystem. However, to date there have been no reports describing hyporheic microbial communities inhabiting high-gradient freestone rivers that predominate in the mountainous western United States.

The objective of the current study was to employ a suite of molecular microbial ecology techniques (DGGE pattern analysis, 16S rDNA phylogeny, and real-time qPCR) to describe the *in situ* community structure and seasonal population dynamics of the microbial hyporheos in different-sized rivers in western Montana. Three rivers representing a range of river types were sampled periodically for more than a year to obtain information regarding: (1) the structure and composition of these microbial communities, (2) the degree of heterogeneity within and between streams, and (3) seasonal trends in the abundance of key bacterial groups.

The data indicate that, while there is little within-stream variation in the composition of microbial communities inhabiting the hyporheic zone, there are marked seasonal changes. These communities primarily contain members of the α-, β-, and γ-proteobacteria, with *Hyphomicrobium* and *Rhizobium*-like 16S rDNA sequences being the most numerically abundant throughout the year. Although total bacterial cell density was relatively constant throughout the year, individual populations exhibited different seasonal abundance patterns.

Materials and Methods

Study Streams

Three streams (Fig. 1A) were sampled five times over thirteen months from September 2000 through October 2001. The streams were selected to represent a range of stream types based on mean base discharge, substratum type, and drainage area (Table 1). The general physical characteristics of each stream throughout the year were obtained from the USGS Montana stream-flow Web site (http://waterdata.usgs.gov/mt/nwis/current?type=flow). All of the sampled reaches were free of major debris and dams and had riparian vegetation dominated by cottonwood groves, alders, and willows. Watershed land use near the sampled reaches included rangeland, hay fields, and some rural residential housing. There were no significant sources of pollutants upstream of any of our sampling locations. Dissolved anions (NO_3^-, PO_4^{3-}, and Cl^-) were measured in surface and porewater for each stream, with water samples taken at the same time as sediment samples ($n = 3$ for each time point). Anion values were determined on a Dionex D500 ion chromatograph as per U.S. EPA method 300.0 using an AS14 anion separation column.

Since there were no significant differences between surface and porewater values ($p > 0.47$), surface water measurements were used as estimates of porewater chemistry to 20 cm depth. The smallest stream, the Little Blackfoot River (LB), was sampled near Garrison, MT (lat. 46 31′11″, long. 112 47′33″) at 1324 m above sea level. The moderately sized stream, Rock Creek (RC), was sampled near Missoula, MT (lat. 46 43′21″, long. 113 40′56″) at 1072 m above sea level. The largest stream, Big Hole River (BH), was sampled near Glen, MT (lat. 45 26′26″, long. 112 33′20″) at 1478 m above sea level.

Sampling design

Approximately 6 L of sediment from each of the three sampled streams were collected by hand-sieving bulk sediment (0–20 cm depth) with stacked 2.36-mm and 1.7-mm stainless steel sieves.

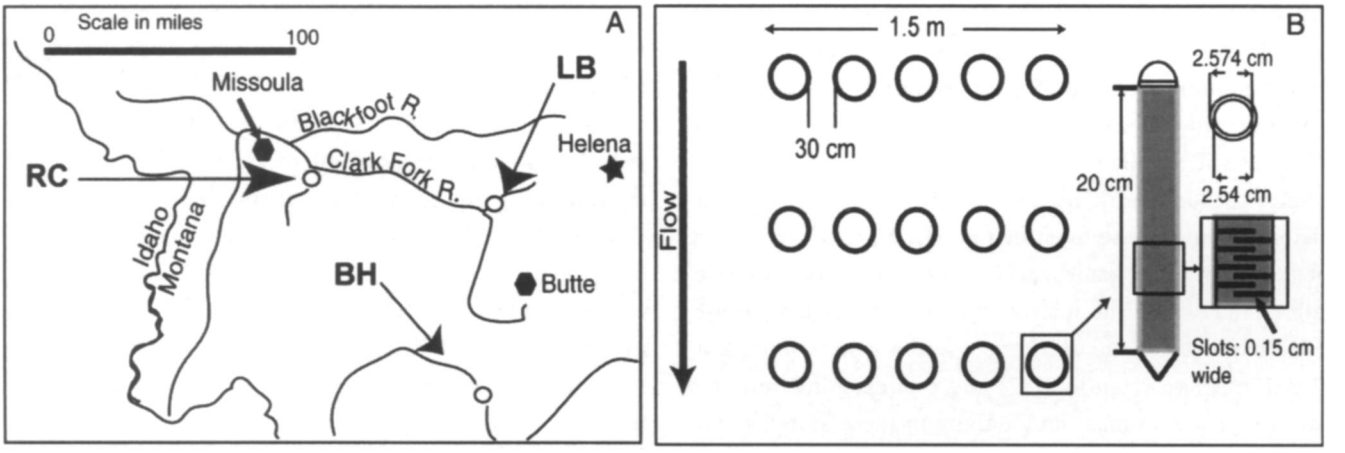

Fig. 1. Sampling sites and sampler design. (A) Map of sampling sites. Each stream sampled is indicated by a ○, LB, Little Blackfoot River, RC, Rock Creek; BH, Big Hole River. (B) Column placement at each stream consisted of groups of 5 replicate columns placed at the head of 3 sequential riffles. The distance between column sets depended on the distribution of the riffles in each stream. Column dimensions are as indicated.

This same size fraction of sediment was analyzed from each stream in order to minimize differences due to physical heterogeneity within streams, and thus maximize our ability to detect differences in microbial communities (inhabiting this same size fraction) between streams. Sediments were bagged in sterile Whirlpak bags (Nasco, Fort Atkinson, WI) and kept on wet ice during transport to the laboratory. Fifteen replicate 125-g samples of sediment from each stream were packed into acid-washed (soaked in 0.1% HCl overnight, then rinsed 3× in Milli-Q water) PVC columns (Fig. 1B). These packed columns were buried vertically (0–20 cm depth) in each of the streambeds in groups of five columns at the heads of three consecutive riffles (Fig. 1B). Placing the columns at the heads of riffles ensured that the porewater at these locations would be dominated by the influx of surface water, thus reducing variability between sampling locations within and between streams due to the potential influx of ground waters. The walls and tops of the columns were constructed of opaque PVC to prevent the influx of light, thus making the column interior more representative of the nonphotic hyporheic zone. Columns were allowed to equilibrate *in situ* for 6 weeks prior to initial sampling on September 10, 2000 (fall). Additional samples were subsequently taken on November 17, 2000 (late fall), April 22, 2001 (spring, pre-runoff), July 1, 2001 (midsummer), and October 2, 2001 (fall). Sampling was not possible during midwinter or the spring runoff period because of overlying ice and hazardous conditions, respectively. For each time point, one column from each of the three groups within each stream was harvested and analyzed (for a total of three replicates from each stream at each time point). The sediments were removed from the PVC cores, gently rinsed on-site with stream water in a 1.7-mm stainless steel sieve, and then placed on dry ice or at −70°C until being lyophilized overnight in a Freezemobile 24 (Amoco Productions Co., Tulsa, OK). Once dried, the sediments were stored at −70°C prior to analysis.

Microscopic Enumeration of Bacteria

Total bacterial cells associated with 1-g samples of lyophilized sediment were enumerated as described previously [23]. One

Table 1. Physical stream parameters[a]

Parameter	LB	RC	BH
Catchment area (sq. miles)	407	885	2,665
Streambed gradient	0.004	0.007	0.003
Base flow rate (c.f.s.)	104.7 (21.4)	181.1 (9.5)	535.6 (40.7)
Predominant bed material	Small cobbles/gravel	Large cobbles/gravel	Large cobbles/gravel
Stream order	3rd	3rd	4th
Avg. pH	8.3	8.1	8.0
Cl^- (μg/mL)	2.35 (0.057)	bdl	3.154 (0.13)
N as NO_3^- (μg/mL)	0.061 (0.035)	0.031 (0.02)	0.017 (0.01)
PO_4^{2-} (μg/mL)	bdl	bdl	bdl

[a] Base flow rates and dissolved anion values are indicated as means (standard error) (n = 3). bdl, Below detection limit (0.1 ppm for Cl^-, 0.05 ppm for PO_4^{2-}).

slide was made for each column sampled, and 30 fields of view or 400 bacterial cells counted from each slide.

DNA Extraction

For bacterial community DNA recovery, 1-g samples of lyophilized sediment were extracted by the method of Yu and Mohn [78] with the following modifications: 0.5 g of sterilized and nuclease-free (baked overnight at 350°C) 0.1-mm zirconia/silica beads (Biospec, Bartlesville, OK) were used. All isopropanol and ethanol precipitations were performed overnight at −20°C. Prior to PCR analysis, 20-μL aliquots of each sample were further purified using Sephadex G-50 spun columns [62]. RNA was removed by treatment with 5 μL of 1 mg/mL RNase A solution (DNase free) for 30 min at 37°C. All glassware was sterilized by autoclaving. The manufacturer certified all disposable plastic-ware as sterilized, DNase-, and RNase-free. Similar bead-beating approaches for the extraction of DNA from environmental samples have been shown to successfully recover DNA sequences from the majority of Bacterial and Archaeal lineages [52, 60, 64].

Denaturing Gradient Gel Electrophoresis and Gel Pattern Analysis

PCR amplification for DGGE analysis was performed using conserved general 16S rDNA primers 536fc and 907r [29] (note that primer 536fc comprises a 40-bp GC clamp (CGC CCG CCG CGC CCC GCG CCC GGC CCG CCG CCC CCG CCCC) at the 5′ end of the 536f primer in this citation). PCR was performed with *Taq* polymerase (Roche Diagnostics, Mannheim, Germany) using the manufacturer's suggested protocol for a standard 25-μL reaction and a PTC-100 thermal cycler (MJ Research Inc., Reno, NV). An initial denaturing step of 5 min at 95°C was performed followed by 35 cycles of 15 s at 95°C, 30 s at 55°C, and 60 s of extension at 72°C, and finally by 5-min extension at 72°C. Generally, the products of four replicate PCR reactions were pooled to provide sufficient PCR products (400 ng) for DGGE analysis.

The PCR amplicons generated from each sample were separated via DGGE using the Bio-Rad D-GENE System (Bio-Rad Laboratories, Hercules, CA). The Gibco 100-bp ladder (Invitrogen Corp., Carlsbad, CA) and a separate lane with 100 ng each of PCR product amplified from chromosomal DNA of *Clostridium perfringens* and *Micrococcus luteus* were included in each gel as positional markers. A linear gradient of denaturant ranging from 25% to 60% (7 M urea: 40% (wt/vol) formamide) in a 6% acrylamide gel matrix was used. Each gel was run at 60°C and 30 V for 30 min, before the voltage was increased to 130 V for 5 h. Following electrophoresis, gels were stained for 2 h at 37°C with a 5× concentration of SyberGreen I (BioWhittaker Molecular Applications, Rockland, ME), and bands were visualized using a Bio-Rad Gel Doc 1000 and Molecular Analyst software (Bio-Rad Laboratories).

GelCompar v.4.0 software (Applied Maths, Kortrijk, Belgium) was used to analyze DGGE images for pattern similarities. All band patterns were normalized to the positional markers in each gel, thereby eliminating variation between individual gels. A similarity index, based on the Dice coefficient $S_D = 2n_{AB}/n_A + n_B$ (where n_A = the number of bands in lane A, n_B = the number of bands in lane B, n_{AB} = the number of common bands between lanes A and B), was calculated by comparing the DGGE pattern from each sample to those from all other samples.

Cloning and Sequencing of DGGE Gel Bands

Bands of interest from the DGGE patterns demonstrating the greatest number of bands (September 2000) were excised, re-amplified, cloned into a plasmid vector, and then subjected to DNA sequence analysis. Bands were excised from the gel using a flame-sterilized razor blade, placed into sterile 500-μL tubes, macerated with a pipette tip, mixed with 100 μL of elution buffer (50 mM KCl, 10 mM Tris, 0.1% Triton X-100, pH 8.0), and then incubated at room temperature overnight to elute the DNA from the gel matrix. PCR products were generated from the eluted bands as described above, purified with Qiaquick PCR Clean-up columns (Qiagen, Valencia, CA) using the manufacturer's suggested protocol, and cloned into the pT7Blue-3 plasmid vector using the Perfectly Blunt Cloning Kit (Novagen, Inc., Madison, WI). Plasmids were harvested from 2-mL, 37°C overnight cultures of *Escherichia coli* using Qiagen mini-prep kits (Qiagen, Valencia, CA) as recommended by the manufacturer. To ensure that plasmid clones contained the sequence of interest, each was used as template for PCR using the 536fc-907r primer pair and the products analyzed by DGGE alongside the original total community PCR products to confirm band position. DNA sequence analysis was performed by MWGBiotech, Inc. (High Point, NC).

Phylogenetic Analysis

DNA sequences were analyzed for completeness and checked for chimeric character using the Ribosomal Database Project (http://rdp.cme.msu.edu/html/http://rdp.cme.msu.edu/html/) Chimera Check function. Any sequences that appeared chimeric were excluded from further analysis. The Sequence Match function of RDP II was used to determine the closest known relative of all recovered sequences. Preliminary alignment of related sequences was performed with the Sequence Align function of RDP II, and then SeqPup v.0.8 (IUbio Archive, http://iubio.bio.indiana.edu/soft/molbio/seqpup/java/) was used to manually align these sequences as needed. Phylogenetic trees were generated from the aligned sequences using Paup v.4.0b.8.a (Sinauer Associates, Inc., Sunderland, MA). Separate trees were generated using neighbor joining, maximum parsimony, and maximum likelihood algorithms. Each tree was bootstrapped 100 times and a consensus tree generated from those trees. The major branches of the consensus tree were used to identify the dominant groups from which group-specific primers were subsequently generated for qPCR analysis.

Table 2. qPCR primer constructs, Tm values, number of matches in RDP, and examples of the species each primer pair detects

Targeted group	Probe name/sequence	Tm	# of matches in RDP	Type species amplified	RDP score
Appendaged bact grp. Product size = 83 nt	Ap Forward primer 2 (5′ - 3′) AACACCAGTGGCGAAGG	59.61	11	*Pirellula staleyi* ATCC 27377	0.637
	Reverse primer 2 (3′ - 5′) GAGCAAACAGGATTAGATACCC	60.81	17	*Hyphomicrobium denitrificans*	0.846
Aquabact/Rhodoferax grp. Product size = 171 nt	AR forward primer 2 (5′ - 3′) CGGYAGAGGGGGATGGAA	62.18	0	*Rhodoferax* unidentified proteobacterium	0.949
	AR Reverse primer 2 (3′ - 5′) CCCTAAACGATGTCAACTGG	60.4	0	*Aquabacterium commune* str. B8	0.922
N-Fixer grp. Product size = 86 nt	Nfix Forward primer F1 (5′ - 3′) CCWGTAGTCCTAGCCGTAA	60.16	0	*Chamaesiphon subglobosus* PCC 7430	0.741
	N fix Reverse Primer 2 (3′ - 5′) CTAACGCGTTAAGTATCCCG	60.4	208	*Nostoc* GSV224 str. GSV224	0.940
Pseudomonad grp Product size = 143 nt	Xn Forward primer 2 (5′ - 3′) GAAATGCGTAGAGATCGGGAG	62.57	0	*Xanthomonas hyacinthi* LMG 739 (T)	0.692
	Xn Reverse Primer 2 (5′ - 3′) ACRTCCAGTTCGCATCGTTTAGG	62.77	133	*Xanthomonas melonis* LMG 8670 (T)	0.841

Real-Time Quantitative PCR (RT-qPCR)

A suite of group-specific primers corresponding to the groups defined by the phylogenetic analysis were designed and used to quantify the abundance and distribution of each group via RT-qPCR. All primer pairs (Table 2) were generated from consensus sequences for each phylogenetic group and tested for self-complementarity (using Mac Vector, International Biotechnologies, Inc., New Haven, CT), secondary structure (using M-fold) [44, 80], and group-level specificity (using the RDP II probe match function, http://rdp.cme.msu.edu/cgis/probematch.cqi?su=SSU) prior to use. Quantitative PCR reactions were performed using a Bio-Rad iCycler (Bio-Rad) and the SyberGreen I detection method. Briefly, each 25-μL PCR reaction contained a 1× concentration of a modified 10× Roche PCR buffer (Roche Diagnostics) (10 mM Tris-HCl, 0.3 mM $MgCl_2$, 50 mM KCl, pH 8.3, 1:10,000 dilution of SyberGreen I), 6.25 mM of each dNTP, 1 pmol of each primer, 7% DMSO, and 1.25 U of *Taq* polymerase (Roche Diagnostics). Separate standards were designed for each targeted phylogenetic group from our clone library. For each phylogenetic group, five clones were restricted with *Not*I (Promega, Madison, WI) using the manufacturer's suggested protocol, and mixed together in equal proportions for use in copy number calibration. The plasmid copy number/μL was determined for each standard mixture (μg of cut standard plasmid mixture/μL · [molecules·bp/1.05×10^{15} μg] · 1/3821 bp per plasmid = # plasmid copies/μL). RT-qPCR reactions were run on serial dilutions of each standard mixture to relate threshold cycle number to copy numbers of the target sequence and to generate standard curves for quantification in unknown samples. Typically, standard curves were linear across five orders of magnitude (10^7–10^2 copies, R^2 = 0.99–0.97). Samples that fell above or below this linear range were diluted or concentrated, respectively, to bring the target copy number into the linear range of detection.

The following PCR conditions were used to quantify the copy number/g for each of the defined phylogenetic groups: Appendaged group (Ap), 5 min at 95°C then 45 cycles of 15 s at 95°C, 30 s at 58.4°C, and 60 s at 72°C; *Aquabacterium*/*Rhodoferax* group (A/R), 5 min at 95°C then 45 cycles of 15 s at 95°C, 30 s at 59.4°C, and 60 s at 72°C; *Nostoc* and *Chamaesiphon* group (N/C), 5 min at 95°C, then 40 cycles of 15 s at 95°C, 30 s at 57.3°C, and 60 s at 72°C; Pseudomonad group (Ps), 5 min at 95°C then 40 cycles of 15 s at 95°C, 30 s at 61.5°C, 60 s at 72°C. Fluorescence based on SyberGreen binding was measured in each cycle after the 72°C extension period.

Statistical Analysis of Data

Univariate analysis of variance (ANOVA) and multivariate analysis of variance (MANOVA) were used to determine statistical differences between means. ANOVA is a statistical test that is used to determine if two means are different from one another with respect to a single independent variable (e.g., time or stream) [26]. MANOVA is a statistical technique related to ANOVA; however, MANOVA can test for differences between the means of two or more dependent variables with respect to multiple independent variables or factors simultaneously [26]. In addition, each test can determine if there is an interaction between the independent variables (represented as stream × time) that affects the dependent variable. Interaction terms found to be significant indicate that both independent factors (stream and time) have a combined effect on the dependent variables (e.g., DGGE pattern similarity between LB and BH, bacterial cell density, or abundance of each phylogenetic group).

Means of DGGE similarity scores, grouped by stream and date, were tested for significant differences ($p < 0.05$). A similarity matrix was generated that contained the mean similarity scores for each stream and date compared to the means of all other streams and dates. A nonmetric dimensional scaling analysis (NMDS) (NCSS, Kaysville, UT) was applied to this mean similarity matrix to determine the relative differences between samples across time, both within and between streams. The

NMDS plot can be interpreted by evaluating the observed distances between points on the graph, or by finding patterns in the multidimensional space of the plot [5, 36]. NMDS has previously been used to analyze geographic genetic structure [41]. When applied to DGGE data, the NMDS plot graphically represents the relative differences between streams at each time point and changes within streams across time. By using the mean similarity matrix to evaluate differences within streams and between streams across time, we reduced the number of data points, thus simplifying interpretation of the NMDS plot.

All statistical tests were performed using NCSS 2001 software (NCSS, Kaysville, UT). A p value of 0.05 was set as the significance threshold for all Tukey–Kramer multiple comparisons tests.

Results

Community Structure Analysis

DGGE analysis was performed to assess and compare microbial community structure within and between streams. Although visual examination of DGGE patterns (data not shown) indicated seasonality in the patterns of the detectable microbial populations, we applied pattern-matching analysis using GelCompar software to better quantify similarities and differences within and between streams. Within-stream heterogeneity was assessed by calculating the means and standard errors of the similarity scores for all replicates and time points for each stream, LB = 96.8 ± 1.05, RC = 96.5 ± 0.88, BH = 97.4 ± 0.67. An analysis of variance (ANOVA) indicated that there was no significant difference in within-stream variability over the entire sampling period ($F_{\text{within stream similarity}} = 0.27$, $p = 0.947$). The mean within-stream similarity values were much higher than the mean similarity values between streams, 96.1% similar vs 80.87% similar, respectively (data not shown). This analysis indicated that there was little variability within a stream during each time point we sampled, but does not confirm the seasonality within streams indicated by visual analysis of DGGE patterns.

Between-stream and between time-point comparisons were performed using NMDS (Fig. 2A). The results suggest that the RC and LB communities were very similar at the 9-00, 11-00, and 4-01 sampling times as indicated by the proximity and positioning of their respective symbols. The BH community, however, was more distinct from the others at these time points as indicated by its relative position in Fig. 2A. During the summer of 2001 (7-01) the RC and LB communities diverged from each other, while the structure of the BH community became more similar to that of LB. The relative similarity of the LB and BH communities was also apparent at the last (fall) sampling time point (10-01), while the RC community on that date had returned to a structure more like that found on the 4-01 sampling date at both LB and RC.

To make an assessment of bacterial species richness, we determined the number of bacterial sequence types (based on DGGE band numbers) at each stream for each sampling time. Although each stream exhibited some differences in the number and position of detectable bacterial sequence types (DGGE bands), the general behavior of the species richness plots is similar among all three streams (Fig. 2B). ANOVA indicated that there were significant differences in the number of detectable bacterial sequence types between streams ($F_{\text{stream}} = 5.74$, $p = 0.011$) and between dates ($F_{\text{date}} = 30.34$, $p < 0.001$). In addition, there was a significant interaction between the number of bacterial sequence types found within each stream and the sampling date ($F_{\text{stream} \times \text{date}} = 4.84$, $p = 0.003$).

Phylogenetic Analysis

To identify the types of organisms comprising the hyporheic microbial communities, several prominent bands from each stream for the September 2000 sampling date were excised from a DGGE gel, cloned, and sequenced (Fig. 3). The sequences obtained were compared to the RDP II database and closest matches to known species determined (Table 3). This analysis revealed that Gram-negative organisms from a number of different genera including *Aquabacterium*, *Chamaesiphon*, *Hyphomicrobium*, *Leptothrix*, *Nostoc*, *Pirellula*, *Planctomyces*, *Rhizobium*, *Rhodoferax*, and *Xanthomonas* dominated these hyporheic bacterial communities.

The DNA sequences were also subjected to phylogenetic analysis to determine whether similar phylogenetic groups inhabited each stream (Fig. 4). Sequences obtained from LB showed the most general distribution throughout the tree (indicating broad representation across phylogenetic groups), while the sequences recovered from BH and RC were more narrowly distributed. Four phylogenetic groups were designated based on the identity of the best matches to known species (Fig. 4.) These include the appendaged (Ap) group represented by *Hyphomicrobium- and Rhizobium*-like sequences, the *Aquabacterium/Rhodoferax* (A/R) group represented by *Aquabacterium*- and *Rhodoferax*-like sequences, the N/C group represented by *Chamaesiphon*- and *Nostoc*-like sequences, and the Pseudomonad group (Ps) represented by *Pseudomonas-*

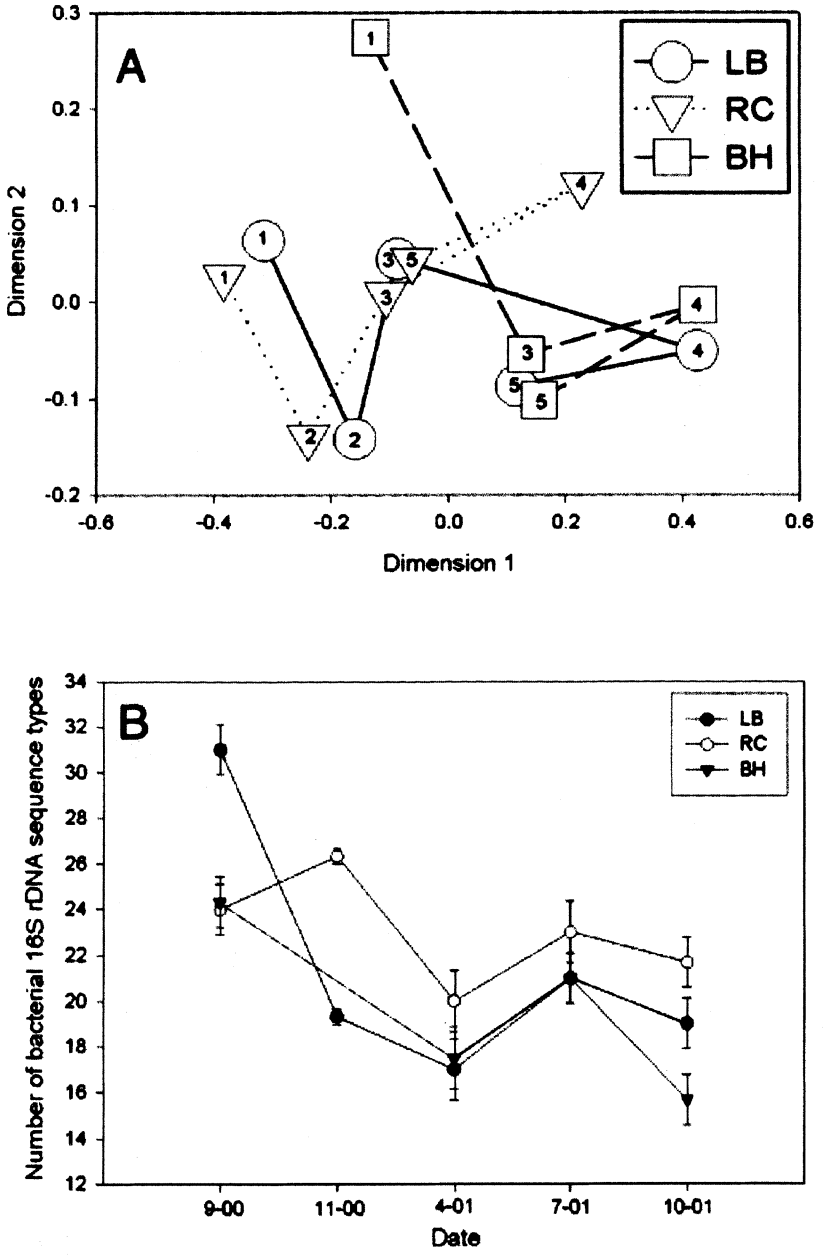

Fig. 2. Bacterial community structure comparisons based on DGGE pattern analysis. (A) Within-stream DGGE pattern similarity averaged over the course of the study (n = 5 for LB and RC, n = 4 for BH). (B) NMDS analysis of the mean similarity matrix indicating relative differences in DGGE pattern similarity within and between streams over time. Numbers within each symbol represent the different sampling time points (1 = 9-00, 2 = 11-00, 3 = 4-01, 4 = 7-01, 5 = 10-01). (B) Richness of bacterial sequence types (i.e., DGGE band number) vs time at all streams (n = 3 for each stream at all time points).

and *Xanthomonas*-like sequences. All of the sequences in each group indicated in Fig. 4 were aligned to derive consensus sequences from which group-specific primers were generated for the RT-qPCR analyses described below.

Seasonal Microbial Population Dynamics

Direct microscopic enumeration was used to estimate total bacterial cell densities in each stream over the course of this study (data not shown). Although variations in bacterial cell densities within and between streams were observed over the course of the year, average bacterial cell densities remained in the range of 10^7–10^8 cell number g^{-1} of sediment. ANOVA indicated that there were significant differences in cell number g^{-1} values among the sampling locations (F_{stream} = 10.19, p = 0.0006) and among sampling dates (F_{date} = 8.96, p = 0.0003), and that cell number g^{-1} values were significantly affected by the interaction between stream and time ($F_{stream \times time}$ = 7.34, p = 0.0002). A post-hoc multiple comparisons test (Tukey-Kramer) indicated that the significance of these relationships was dependent primarily on only three of the 15 sample sets analyzed (LB 11-00, RC 11-00, and RC 7-01).

Differences in phylogenetic group abundance between streams, and time points were assessed using RT-qPCR. To determine if there were significant differences among

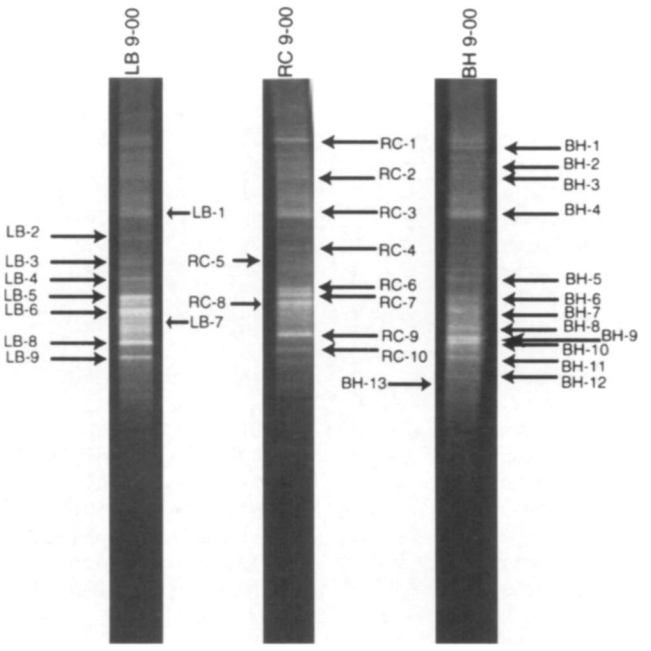

Fig. 3. DGGE lanes from 9-00 samples indicating which bands were excised and cloned for DNA sequence analysis. Arrows indicate excised bands and are labeled with the same names assigned to the recovered sequences.

any of the response variables (copy numbers g^{-1} of each of the phylogenetic groups) a MANOVA was performed using stream and sampling time as the factors. In addition, we tested for a significant interaction between the two factors (stream × time). This analysis indicated there were significant differences in the abundance of each of the monitored phylogenetic groups across time (Wilks Lambda $F_{date} = 7.64$, $p = 0.003$), but no differences between streams (Wilks Lambda $F_{stream} = 1.46$, $p = 0.33$), nor was there a significant interaction between the two factors (Wilks Lambda $F_{stream \times time} = 0.94$, $p = 0.62$). Based on these results only sampling time was considered as a factor for further analyses. A plot of the mean and standard error of each phylogenetic group for all streams illustrates the common seasonal pattern found among all of the phylogenetic groups at all three streams revealed by the MANOVA results (Fig. 5).

ANOVA indicated that there were significant differences in the abundance of all of the phylogenetic groups across time (Ap group $F_{date} = 9.26$, $p < 0.0001$; A/R group $F_{date} = 6.62$, $p = 0.001$; N/C group $F_{date} = 4.33$, $p = 0.01$; Ps group $F_{date} = 8.96$, $p = 0.0001$). The abundance of the Ap group ranged between 7.76×10^7 and 2.57×10^9 copy numbers/g for the summer (7-01) and fall (10-01) sampling dates, respectively. This group was the most numerically abundant of all the groups measured, with average copy numbers g^{-1} one to two orders of magnitude greater than for the other three groups. The A/R group exhibited perhaps the most striking seasonal variation in copy number g^{-1}. This group was most abundant during late summer and fall (7-01 and 10-01 sampling dates) with average copy numbers g^{-1} reaching as high as 5.12×10^7. Similar to the N/C and Ps groups, this group had its lowest population density during the late winter/early spring (4-01 sampling date) with average copy numbers of 1.15×10^5 g^{-1}. The estimated abundance of the N/C group was similar to that of the A/R group; however, the seasonal variation in the N/C group was less dramatic. The highest population numbers for the N/C group were seen during the fall (10-01) with mean copy numbers of 1.25×10^7 g^{-1}, whereas the lowest numbers were observed in late winter/early spring (4-01) with a mean value of 9.12×10^5 copies g^{-1}. The fourth group (Ps) exhibited a seasonal pattern similar to that observed for the A/R and N/C groups. The largest population size of this group was measured during fall (9-00) with mean copy numbers equal to 7.94×10^6 g^{-1}, while the smallest population size was found during late winter/early spring (4-01) when mean copy numbers had decreased to 7.24×10^4 g^{-1}.

Discussion

Seasonal patterns in microbial community structure have previously been noted in a variety of systems [4, 13, 15, 38, 53, 61, 66, 67]. A number of factors including grain size [7, 37], the quantity and quality of organic matter (OM) [73, 79], grazing, and predation/viral lysis [34, 65, 71, 74, 76] can influence microbial community structure. Grain size can alter community structure through its effects on flow rates [77] and the quality and quantity of available nutrients [9]. Therefore, we sampled a single size fraction of sediment within each stream to control for the effects of physical heterogeneity and grain size on bacterial community structure. It must be acknowledged that this experimental design potentially reduced the ability to detect the total hyporheic community diversity if different populations or species are associated with different sediment fractions. However, this powerful approach, based on managing within-stream physical heterogeneity, allowed us to detect significant differences in group-level abundance and community composition between different streams and at different times throughout the year. DOC

Table 3. Sequence Identities of the excised DGGE bands that appear in Fig. 3

Band	Best match in RDP database	Group level affiliation	Sab score	Accession number
LB-1	*Leptothrix* MBIC3364 Str. MBIC3364	β-Proteobaoteria	0.887	AB015048
LB-2	*Holophaga*/Acidobacterium bacterial species 16S rRNA gene (clone 11-25)	Holophaga/Acidobacterium	0.725	BSPZ95709
LB-3	*Chamaesiphon subglobosus* PCC 7430	Cyanobacteria	0.741	Chms.sglbs
LB-4	*Nostoc* GSV224 str. GSV224	Cyanobacteria	0.94	AF062637
LB-5	*Geobacter* sp. str. JW-3	δ-Proteobacteria	0.97	AF019932
LB-6	*Azospirillum doebereinerae* str. 63f	β-Proteobacteria	0.62	AJ238567
LB-7	*Aquabacterium commune* str. B8	α-Proteobacteria	0.922	Aqa.commun
LB-8	Alpha-proteobacterium isolate from a sludge community (*Rhizobium-Agrobacterium* group)	α-Proteobacteria	0.814	AF072927
LB-9	Alpha-proterobacterium unidentified eubact. (*Rhizobium-Agrobacterium* group)	α-Proteobacteria	0.815	UEU68615
RC-1	*Acidovorax* G8B1 str. G8B1	β-Proteobacteria	0.881	AJ012071
RC-2	*Comamonas* sp. 163 rRNA gene, isolate 158	β-Proteobacteria	0.889	CSPAJ2803
RG-3	*Rhodoferax* unidentified proteobacterium arc53	β-Proteobacteria	0.931	U76105
RC-4	*Leptothrix* MBIC3364 Str, MBIC3364	β-Proteobacteria	0.894	AB015048
RC-5	*Xanthomonas melonis* LMG 8670 (T)	γ-Proteobacteria	0.841	Xan.meloni
RC-6	*Frafeuria aurantia* IFO 3245 (T)	γ-Proteobacteria	0.749	Frt.aurant
RC-7	Acidobacterium subdivision, Mount Coot-tha region 5–10 cm depth soil DNA clone MC 26	γ-Proteobacteria	0.719	env.MC26
RC-8	Beta-proteobacterium, Nitrosomonas Multiformis sub-group: 1428 clone S28	β-Proteobacteria	0.812	AF072922
RC-9	*Aquabacterium commune* str. B8	β-Proteobacteria	0.942	Aqa.commun
RC-10	*Hyphomicrobium denitrificans* str. X DSM 1869 (T)	α-Proteobacteria	0.846	Hyp.dnitri
BH-1	Unidentified soil eubacterium from eastern Amazonia (*Actinomadura* subgroup)	High G + C gram positive	0.665	UEU68669
BH-2	*Rhizobium* CJ5 Str. CJ5, 24N USDA 3398	α-Proteobacteria	0.845	Rhb.spCJ5
BH-3	*Planctomyces* sp. str. Schlesner 642	Planctomycetales	0.741	Pln.spS642
BH-4	Nitrospira Moscoviensis sub-group: clone 1405-19	Nitrospira group	0.839	AJ007652
BH-5	Nitrospira Moscoviensis sub-group: clone 1405-19	Nitrospira group	0.859	AJ007652
BH-6	Rhodoferax unidentified proteobacterium arc53	β-Proteobacteria	0.904	U76105
BH-7	Gram positive, high G + C, Acidomicrobium Ferrooxidans subgroup; clone Sva0996	High G + C gram positive	0.668	AJ241005
BH-8	*Pirellula Stalevi* ATCC 27377	Planctomycetales	0.637	Pir.staley
BH-9	Delta-proteobacteria Myxobacieria Pol. Cellulosum sub-group: 1412 str. SHI-1	δ-Proteobacteria	0.794	AB016469
BH-10	*Pelobacter carbinolicus* str. GraBd1 DSM 2380 (T)	δ-Protaobacteria	0.624	Peb.carbi2
BH-11	*Janibacter thuringensis* DSM 11141	High G + C gram positive	0.923	Jan.limosu
BH-12	Uncultured eubacterium (Chloroflexaceae/Deinococcaceae group)	Gram positive	0.534	AF005747
BH-13	Nitrospina sub-group clone C112 (isolated from arid southwestern soil)	Nitrospina subdivision	0.842	env.AzC112

values were below our limit of detection in the sampled streams [49], and the determination of grazing and predation rates was beyond the scope of this investigation. Therefore we are unable to directly address the relationship between these environmental factors and the observed changes in the hyporheic microbial community structure. Instead we focus the discussion on comparing and contrasting these findings to previous studies of bacterial communities in aquatic systems. To facilitate this discussion we provide a brief description of the techniques employed, the type of information each provides, and how these data can be interpreted.

A suite of molecular methods was utilized to describe the seasonal community dynamics within and between three high-gradient streams in the western U.S. DGGE and NMDS were employed to determine differences and monitor changes in microbial community composition between streams and within streams across time. These data are useful for monitoring the presence and absence of species; however, they do not provide information regarding the abundance of individual species or phylogenetic groups or the density of bacterial cells in general. To address these aspects of community change, we employed RT-qPCR using group-specific PCR primers and direct microscopic

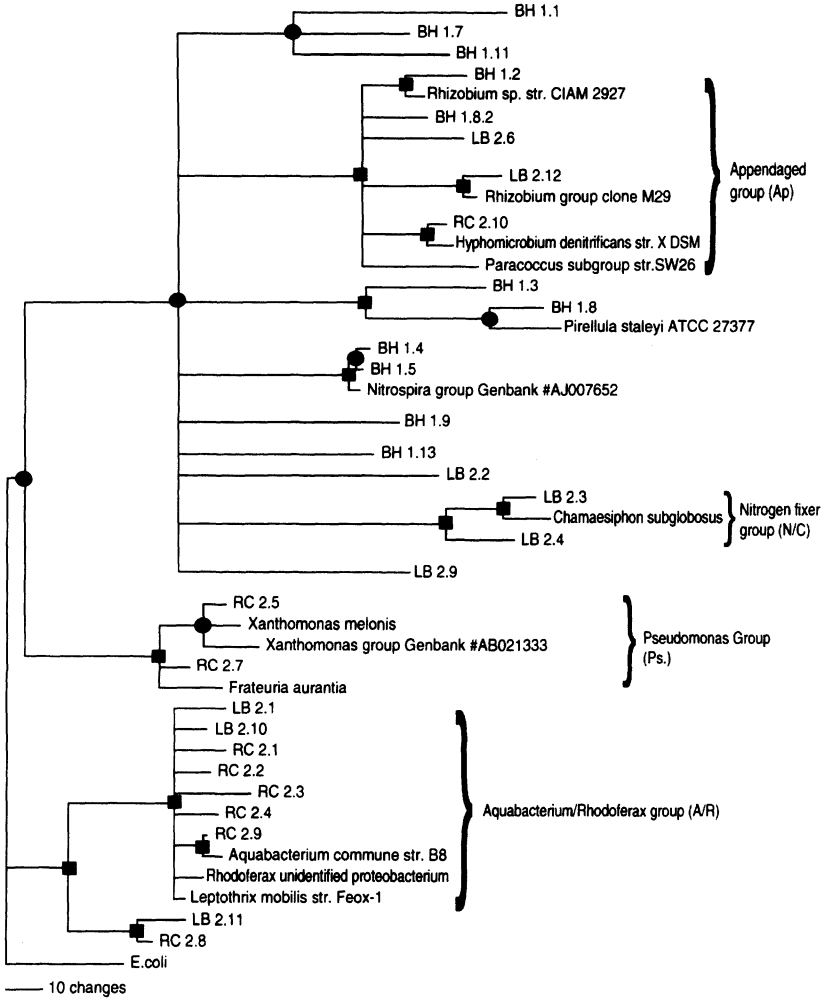

Fig. 4. Consensus phylogenetic tree of partial 16S rDNA sequences amplified with the 536f and 907r 16S primers. The symbols and represent branches that are supported by maximum likelihood, maximum parsimony, and neighbor joining analysis with the following bootstrap values (x), ● = $50 < x < 74\%$, ■ = $x > 74\%$. Refer to Table 3 for clone identities.

enumeration, respectively. Phylogenetic analysis was used to determine group-, genus-, and species-level affiliations of the sequences recovered from the sampled streams. Each of the mechanistically different techniques employed here provides a unique level of resolution for assessing changes in microbial community structure, and results from different approaches are thus often not directly comparable. Therefore, we discuss the data provided by each technique in turn, followed by a summation that merges all of the data into a coherent picture of the seasonal dynamics of the hyporheic microbial community.

Community Composition

Previous studies have utilized NMDS to provide statistical support for DGGE-based estimations of change in microbial community structure due to viral lysis [73] and protozoan grazing [72]. In the current study, NMDS was employed in a similar fashion to graphically represent differences in hyporheic microbial community structure between streams and changes across time. The DGGE analysis revealed that the hyporheic communities sampled were relatively homogenous within the sampled reaches of each stream. However, there were significant changes in the community composition across time.

In addition to community structure comparisons, these data demonstrated that the number of detectable bacterial sequence types (DGGE bands) found in the samples fluctuated during the study (Fig. 2B). Since some bacteria have multiple, slightly divergent copies of rRNA genes [35], it is difficult to accurately determine bacterial species richness *in situ* based solely on DGGE analysis. However, the number of bacterial sequence types in a sample has previously been used as an estimate of bacterial species richness in aquatic and terrestrial systems [73, 79]. Thus, not only does the composition of the hyporheic bacterial community change throughout the year (Fig. 2A), but so apparently does the richness of the community (Fig. 2B).

Since there are no previous descriptions of hyporheic microbial communities using DGGE and NMDS, a direct

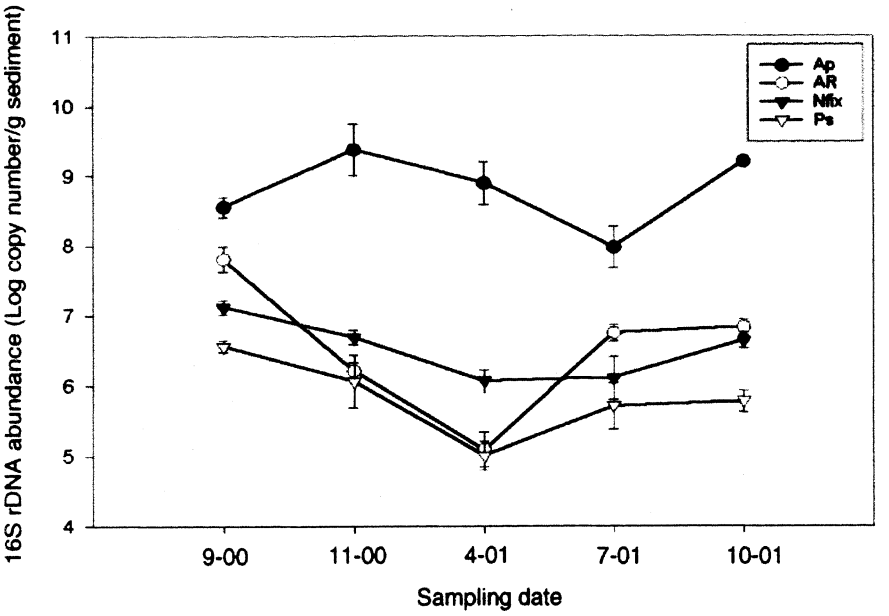

Fig. 5. Means and standard errors (n = 3) of phylogenetic group abundance averaged across all streams versus sampling time. Note that 16S rDNA copy number/g values are plotted on a logscale. Ap, Ap group 16S rDNA copy # g^{-1}; A/R, A/R group 16S rDNA copy # g^{-1}; Nfix, Nfix group 16S rDNA copy # g^{-1}; Ps, Ps group 16S rDNA copy # g^{-1}.

comparison of our data with previous findings is not possible. However, the phylogenetic analysis, bacterial cell densities, and group-level abundance data presented here can be related to other investigations of sediment-associated and pelagic aquatic bacterial communities.

Phylogenetic Data

The majority of the recovered sequences were most closely related to Gram-negative heterotrophic bacteria known to inhabit aquatic environments. Most of the genera represented in the clone library can form biofilms, which would allow them to attach and maintain resident populations in flowing systems like these stream environments. The Ap group consisted of *Hyphomicrobium*- and *Rhizobium*-like sequences. *Hyphomicrobium* is a common inhabitant of aerobic fresh water environments that frequently attaches to surfaces and may account for up to 25% of the total bacterial community in nutrient-poor water [10]. *Rhizobium* is most commonly associated with soil environments. The *Rhizobium*-like sequences obtained in this study could either be of terrestrial origin (e.g., from runoff) or represent aquatic organisms related to *Rhizobium*. Indeed, *Rhizobium*-like populations have previously been reported in mine tailings in river drainages in western Montana [42].

The A/R group included closest matches to the genera *Aquabacterium*, *Comamonas*, *Leptothrix*, and *Rhodoferax*. Although not previously observed in the hyporheic zone, these organisms are widely distributed in aquatic environments [28, 53, 54, 70]. The N/C group consists of *Nostoc*- and *Chamaesiphon*-like sequences. Some *Nostoc* species are able to grow as dark heterotrophs [59], and *Nostoc*-like species have been found associated with benthic sediments and growing attached to natural substrates in both lotic and lentic environments [30]. The genus *Chamaesiphon* is known to live attached to sediments in aquatic environments and can survive through heterotrophic metabolism [30]. Further, cyanobacteria are ubiquitous in streambeds, and it is thus not surprising to detect them in sediments from the shallow hyporheic zone (0–20 cm depth). The Ps group is comprised of sequences most closely related to *Frateuria* and *Xanthomonas*. *Xanthomonas* species are commonly found in aquatic environments [32], whereas *Frateuria* sp. (previously classified as *Acetobacter*) are more commonly found in terrestrial environments [12]. Both can live as chemoheterotrophs and metabolize a wide array of carbon compounds [30].

These four phylogenetic groupings, into which the majority of recovered sequences fall, represent a wide range of species typically found in aquatic environments [30]. Collectively, these phylogenetic data indicate a microbial community dominated by Gram-negative chemoorganoheterotrophs, a description that fits the model of a hyporheic food web predominantly supported by the entrainment of exogenous organic matter or by a continual supply of DOM [1, 17, 50].

Seasonal Microbial Population Dynamics

DGGE band intensity has previously been used as a relative measure of population densities [31, 45, 66]. However, there are concerns with this approach due to the potential for PCR bias [3, 69]. To mitigate this concern, a RT-qPCR assay was designed to determine the relative abundance of selected phylogenetic groups. All RT-qPCR data are presented as 16S rDNA copy number g^{-1} of sediment since we are unsure of *rrn* operon copy number in these populations. However, for the groups being monitored, the average *rrn* copy number is 2–3 copies/cell [35]. Since a dynamic range spanning one to two orders of magnitude in rDNA copy numbers was observed, we conclude that substantial fluctuations in population abundance occur seasonally.

A protective MANOVA analysis was employed to determine whether there were consistent and significant differences between streams, and whether there were seasonal patterns in the abundance of any of the phylogenetic groups. This type of protective multivariate analysis must be performed prior to analyzing individual response variables because each response variable cannot be assumed to be independent of the others [63]. The lack of significant differences between streams for any of the RT-qPCR response variables suggests that these data represent an estimate of general population dynamics within a variety of sizes of this type of stream. Further, phylogenetic analysis of these sequences demonstrated that, although each stream contains a unique complement of species, the organisms are closely related and readily fall into the recognized groups used in this study. Since these three streams span a breadth of key physical, hydrological, and geochemical parameters, it is reasonable to think that other free-stone streams that fall within these bounding parameters will support a similar complement of species and groups, at least in this geographical region.

Previous work has suggested that standing stocks of bacteria in streams can vary with respect to season [18, 19, 27, 39, 40]. Although the current study also detected a significant interaction between bacterial cell number g^{-1} of sediment and season for three of the 15 sample sets, it should be noted that all cell number g^{-1} values from all locations and time points responsible for that interaction were between 0 and 0.5 log units of all other samples. Considering the inherent variability in data generated by direct enumeration of bacteria on sediments [33], we conclude that there were no biologically relevant differences between streams or time points in total bacterial cell densities as indicated by direct microscopic enumeration. Thus, it appears that standing bacterial cell density is stably maintained throughout the year in these hyporheic environments.

Although little variation in bacterial cell densities was observed, analysis of group-specific 16S rDNA copy numbers/g of sediment indicated that the distribution of the hyporheic bacterial populations did change with respect to season. MANOVA analysis indicated that there were significant differences in 16s rDNA copy number/g of sediment across time. Further, ANOVAs performed after the multivariate MANOVA demonstrated clear seasonal patterns in the abundance of four separate phylogenetic groups found in the hyporheic zone.

Previous investigations in aquatic ecosystems have demonstrated similar seasonal trends in individual phylogenetic group abundance while total bacterial abundance remained relatively constant [2, 8, 24, 25, 53]. Additionally, each of those previous studies indicated that the monitored aquatic bacterial communities consisted predominantly of β-proteobacteria with lower abundances of α- and γ-proteobacteria and the Cytophaga/Flavobacterium cluster. The current survey was based on the detection of individual microbial species by 16S rDNA phylogeny using highly conserved primers (i.e., cloning and sequencing of partial 16S rRNA genes) rather than by probing at the division level as in those prior studies and thus may not be directly comparable. However, if the group level delineations (Ap, A/R, Ps, and N/C) of the RT-qPCR primers employed here are extended to encompass the broader phylogenetic groups in which they reside (i.e., α-, β-, and γ-proteobacteria and Cyanobacteria, respectively), then the group-level abundance data in the current study is in contrast to these previous works. Our data indicate that the hyporheic zone in these streams is dominated by α-proteobacteria rather than the β-proteobacteria throughout the year. Additionally, members of the γ-proteobacteria were as abundant as the β-proteobacteria, and the Cytophaga/Flavobacterium group was not detected. However, since the group-level PCR primers employed were based on the sequence database from the current study and not an exhaustive analysis of available sequences from these larger phylogenetic groupings, it may be inappropriate to directly compare our findings to other studies based on different

rivers and river compartments using mechanistically different approaches.

To the best of our knowledge the current study represents the first description of hyporheic microbial communities inhabiting high-gradient streams of the mountainous west. Collectively, these data support five conclusions regarding microbial communities in hyporheic environments: (1) Each stream supports a unique complement of related species that are subject to seasonal variations; (2) there is low variability in the bacterial species composition within a given reach in any stream if grain size is controlled for; (3) bacterial cell densities are relatively constant, while the constituent populations seasonally fluctuate over orders of magnitude; (4) the seasonal fluctuations in group-level abundance are common between streams; and (5) hyporheic microbial communities in the streams studied are dominated by α-proteobacteria rather than β-proteobacteria as seen in other types of aquatic microbial communities. These observations may be useful in predicting seasonal fluctuations in hyporheic microbial community structure in similar environments, and in detecting the effects of anthropogenic contaminants on intact lotic ecosystems. In addition, the approaches presented here may assist in exploring the effects of DOM quality and quantity, grazing pressure, viral lysis, and other environmental factors on hyporheic microbial community structure.

Acknowledgements

We thank Johnnie N. Moore for his valuable input on the experimental design and Justin Harris for his assistance placing sediment samplers and gathering the dissolved anion data. This research was funded by EPA EPSCoR grant No. R-82940001-0.

References

1. Baker MA, Dahm CN, Valett HM (1999) Acetate retention and metabolism in the hyporheic zone of a mountain stream. Limnol Oceanogr 44:1530–1539
2. Battin TJ, Wille A, Sattler B, Psenner R (2001) Phylogenetic and functional heterogeneity of sediment biofilms along environmental gradients in a glacial stream. Appl Environ Microbiol 67:799–807
3. Becker S, Boger P, Oehlmann R, Ernst A (2000) PCR bias in ecological analysis: a case study for quantitative *Taq* nuclease assays in analyses of microbial communities. Appl Environ Microbiol 66:4945–4953
4. Böckelmann DBU (2001) Description and characterization of bacteria attached to lotic organic aggregates (river snow) in the Elbe River of Germany and the South Saskatchewan River of Canada. Dissertation. Technischen Universität Berlin, Berlin, Germany
5. Borg I, Lingoes J (1987) Mulitdimensional Similarity Structure Analysis. Springer Verlag, New York
6. Boulton A, Findlay S, Marmonier P, Stanley E, Valett H (1998) The functional significance of the hyporheic zone in streams and rivers. Annu Rev Ecol Syst 29:59–81
7. Brugger A, Wett B, Kolar I, Reitner B, Herndl G (2001) Immobilization and bacterial utilization of dissolved organic carbon entering the riparian zone of the alpine Enns River, Austria. Aquat Microb Ecol 24:129–142
8. Brummer IHM, Fehr W, Wagner-Dobler I (2000) Biofilm community structure in polluted rivers: abundance of dominant phylogenetic groups over a complete annual cycle. Appl Environ Microbiol 66:3078–3082
9. Brunke M, Gonser T (1997) The ecological significance of exchange processes between rivers and ground water. Freshwat Biol 37:1–33
10. Corpe WA, Jensen TE (1996) The diversity of bacteria, eukaryotic cells and viruses in an oligotrophic lake. 46:622–630
11. Craft J, Stanford J, Pusch M (2002) Microbial respiration within a floodplain aquifer of a large gravel-bed river. Freshwat Biol 47:251–261
12. Duineveld BM, Kowalchuk GA, Keijzer A, Van Elsas JD, Van Veen JA (2001) Analysis of bacterial communities in the rhizosphere of *Chrysanthemum* via denaturing gradient gel electrophoresis of PCR-amplified 16S rRNA as well as DNA fragments coding for 16S rRNA. Appl Environ Microbiol 67:172–178
13. Edwards KJ, Gihring TM, Banfield JF (1999) Seasonal variations in microbial populations and environmental conditions in an extreme acid mine drainage environment. Appl Environ Microbiol 65:3627–3632
14. Fellows C, Valett H, Dahm C (2001) Whole-stream metabolism in two montane streams: contribution of the hyporheic zone. Limnol Oceanogr 46:523–531
15. Ferris M, Ward D (1997) Seasonal distributions of dominant 16S rRNA-defined populations in a hot spring microbial mat examined by denaturing gradient gel electrophoresis. Appl Environ Microbiol 63:1375–1381
16. Findlay S (1995) Importance of surface-subsurface exchange in stream ecosystems: the hyporheic zone. Limnol Oceanogr 40:159–164
17. Findlay S, Strayer D, Goumbala C, Gould K (1993) Metabolism of streamwater dissolved organic carbon in the shallow hyporheic zone. Limnol Oceanogr 38:1493–1499
18. Findlay S, Tank J, Dye S, Valett HM, Mulholland PJ, Mcdowell WH, Johnson SL, Hamilton SK, Edmonds J, Dodds WK, Bowden WB (2002) A cross-system comparison of

bacterial and fungal biomass in detritus pools of headwater streams. Microb Ecol 43:55–66
19. Fischer H, Pusch M (2001) Comparison of bacterial production in sediments, epiphyton and the pelagic zone of a lowland river. Freshwat Biol 46:1335–1348
20. Fischer HM, Pusch M, Schwoerbel J (1996) Spatial distribution and respiration of bacteria in stream-bed sediments. Arch Hydrobiol 137:281–300
21. Fowler R, Death R (2001) The effect of environmental stability on hyporheic community structure. Hydrobiologia 445:85–95
22. Franken R, Storey R, Williams D (2001) Biological, chemical and physical characteristics of downwelling and upwelling zones in the hyporheic zone of a north-temperate stream. Hydrobiologia 444:183–195
23. Frazar CF (2002) Microbial community production and tolerance in heavy metals polluted sediment. Master's thesis. The University of Montana, Missoula, MT
24. Glockner FO, Fuschs BM, Amann R (1999) Bacterioplankton compositions of lakes and oceans: a first comparison based on fluorescence in situ hybridization. Appl Environ Microbiol 65:3721–3726
25. Glockner FO, Zaichikov E, Belkova N, Denissova L, Pernthaler J, Pernthaler A, Amann R (2000) Comparative 16S rRNA analysis of lake bacterioplankton reveals globally distributed phylogenetic clusters including an abundant group of Actinobacteria. Appl Environ Microbiol 66:5053–5065
26. Hair JF, Anderson RE, Tatham RL, Black WC (1992) Multivariate Data Analysis with Readings, 3rd ed. Macmillan Publishing Company, New York
27. Halda-Alija L, Hendricks SP, Johnston TC (2001) Spatial and temporal variation of Enterobacter genotypes in sediments and the underlying hyporheic zone of an agricultural stream. Microb Ecol 42:286–294
28. Hofle MG, Haas H, Dominik K (1999) Seasonal dynamics of bacterioplankton community structure in a eutrophic lake as determined by 5S rRNA analysis. Appl Environ Microbiol 65:3164–3174
29. Holben WE, Williams P, Saarinen M, Särkilahti LK, Apajalahti JHA (2002) Phylogenetic analysis of intestinal microflora indicates a novel mycoplasma phylotype in farmed and wild salmon. Microb Ecol 44:175–185
30. Holt JG, Krieg NR, Sneath PHA, Staley JT, Williams ST (1994) Bergey's Manual of Determinative Bacteriology, 9th ed. Williams and Wilkins, Baltimore
31. Jackson CR, Churchill PF, Roden EE (2001) Successional changes in bacterial assemblage structure during epilithic biofilm development. Ecology 82:555–566
32. Kawai M, Matsutera E, Kanda H, Yamaguchi N, Tani K, Nasu M (2002) 16S ribsomal DNA-based analysis of bacterial diversity in purified water used pharmaceutical manufacturing processes by PCR and denaturing gradient gel electrophoresis. Appl Environ Microbiol 68:699–704
33. Kepner Jr R, Pratt J (1994) Use of fluorochromes for direct enumerations of total bacteria in environmental samples: past and present. Microbiol Rev 58:603–615
34. Kinner NE, Harvey RW, Blakeslee K, Novarino G, Meeker LD (1998) Size-selective predation on groundwater bacteria by nanoflagellates in an organic-contaminated aquifer. Appl Environ Microbiol 64:618–625
35. Klappenbach JA, Dunbar JM, Schmidt TM (2000) rRNA operon copy number reflects ecological strategies of bacteria. Appl Environ Microbiol 66:1328–1333
36. Kruskal JB, Wish M (1978) Multidimensional Scaling. Sage Publications, Beverly Hills, CA
37. Lee WJ, Patterson DJ (2002) Abundance and biomass of heterotrophic flagellates, and factors controlling their abundance and distribution in sediments of Botany Bay. Microb Ecol 43:467–481
38. Leff LG, Leff AA, Lemke MJ (1998) Seasonal changes in planktonic bacterial assemblages of two Ohio streams. Freshwat Biol 39:129–134
39. Lemke MJ, Brown BJ, Leff LG (1997) The response of three bacterial populations to pollution in a stream. Microb Ecol 34:224–231
40. Lemke MJ, Leff LG (1999) Bacterial populations in an anthropogenically disturbed stream: comparison of different seasons. Microb Ecol 38:234–243
41. Lessa EP (1990) Multidimensional analysis of geographic genetic structure. Syst Zool 39:242–252
42. Macur R, Wheeler J, Mcdermott T, Inskeep W (2001) Microbial populations associated with the reduction and enhanced mobilization of arsenic in mine tailings. Environ Sci Technol 35:3676–3682
43. Malard F, Ward JV, Robinson CT (1999) An expanded perspective of the hyporheic zone. Verh Internat Verein Limnol 27:1–7
44. Mathews DH, Sabina J, Zuker M, Turner DH (1999) Expanded sequence dependence of thermodynamic parameters improves prediction of RNA secondary structure. J Mol Biol 288:911–940
45. Mccaig AE, Glover LA, Prosser JI (2001) Numerical analysis of grassland bacterial community structure under different land management regimens by using 16S ribosomal DNA sequence data and denaturing gradient gel electrophoresis banding patterns. Appl Environ Microbiol 67:4554–4559
46. Mermillod-Blondin F, Creuze Des Chatelliers M, Marmonier P, Dole-Olivier MJ (2000) Distribution of solutes, microbes and invertebrates in river sediments along a riffle-pool-riffle sequence. Freshwat Biol 44:255–269
47. Mulholland PJ, Marzolf ER, Webster JR, Hart DR, Hendricks SP (1997) Evidence that hyporheic zones increase heterotrophic metabolism and phosphorous uptake in forest streams. Limnol Oceanogr 42:443–451
48. Naegeli MW, Uehlinger U (1997) Contribution of the hyporheic zone to ecosystem metabolism in a prealpine gravel-bed river. J N Am Benthol Soc 16:794–804

49. Nagorski SA (2001) Spatial and temporal variation in the geochemistry of several western Montana streams and rivers. Dissertation. The University of Montana, Missoula, MT
50. Naiman RJ, Melillo JM, Lock MA, Ford TE, Reice SR (1987) Longitudinal patterns of ecosystem processes and community structure in a subarctic river continuum. Ecology 68:1139–1156
51. Olsen D, Townsend C, Matthaei C (2001) Influence of reach geomorphology on hyporheic communities in a gravel-bed stream. N Z J Mar Freshwat Res 35:181–190
52. Orphan VJ, Hinrichs K-U, Ussler III W, Paull CK, Taylor LT, Sylva SP, Hayes JM, Delong EF (2001) Comparative analysis of methane-oxidizing Archaea and sulfate-reducing bacteria in anoxic marine sediments. Appl Environ Microbiol 67:1922–1934
53. Pernthaler J, Glockner F-O, Unterholzner S, Alfreider A, Psenner R, Amann R (1998) Seasonal community and population dynamics of pelagic bacteria and Archaea in a high mountain lake. App Environ Microbiol 64:4299–4306
54. Pernthaler J, Posch T, Simek K, Vrba J, Pernthaler A, Glockner FO, Nubel U, Psenner R, Amann R (2001) Predator-specific enrichment of Actinobacteria from a cosmopolitan freshwater clade in mixed continuous culture. Appl Environ Microbiol 67:2145–2155
55. Pusch M (1997) Community respiration in the hyporheic zone of a riffle-pool sequence. In: Gilbert J, Mathieu J, Fournier F (Eds.) Groundwater/Surface Water Ecotones: Biological and Hydrological Interactions and Management Options. Cambridge University Press, Cambridge, UK, pp 51–56
56. Pusch M (1999) The metabolism of organic matter in the hyporheic zone of a mountain stream, and its spatial distribution. Hydrobiologia 323:107–118
57. Pusch M, Fiebig D, Brettar I, Eisenmann H, Ellis BK, Kalpan LA, Lock MA, Naegeli MW, Traunspurger W (1988) The role of micro-organisms in the ecological connectivity of running waters. Freshwat Biol 40:453–495
58. Pusch M, Schwoerbel J (1994) Community respiration in hyporheic sediments of a mountain stream (Steina, Black Forest). Arch Hydrobiol 130:35–52
59. Rippka R, Deruelles J, Waterbury JB, Herdman M, Stanier RY (1979) Generic assignments, strain histories and properties of pure cultures of Cyanobacteria. J Gen Microbiol 111:1–61
60. Ritchie NJ, Schutter ME, Dick RP, Myrold DD (2000) Use of length heterogeneity PCR and fatty acid methyl ester profiles to characterize microbial communities in soil. Appl Environ Microbiol 66:1688–1675
61. Rooney-Varga J, Devereux R, Evans R, Hines M (1997) Seasonal changes in the relative abundance of uncultivated sulfate-reducing bacteria in a salt marsh sediment and in the rhizosphere of *Spartina alterniflora*. Appl Environ Microbiol 63:3895–3901
62. Sambrook J, Fritsch EF, Maniatis T (1989) Molecular Cloning, a Laboratory Manual, 2nd ed. Cold Spring Harbor Laboratory Press, Cold Spring Harbor, NY
63. Scheiner SM (1993) MANOVA: multiple response variables and multispecies interactions. In: Scheiner SM, Gurevitch J (Eds.) Design and Analysis oncological Experiments Chapman and Hall, New York, pp 94–112
64. Sekiguchi H, Watanabe M, Nakahara T, Xu B, Uchiyama H (2002) Succession of bacteria community structure along the Changjiang River determined by denaturing gradient gel electrophoresis and clone library analysis. Appl Environ Microbiol 68:5142–5150
65. Simek K, Pernthaler J, Weinbauer MG, Hornal K, Dolan JR, Nedoma J, Masin M, Amann R (2001) Changes in bacterial community composition and dynamics and viral mortality rates associated with enhanced flagellate grazing in a mesoeutrophic reservoir. Appl Environ Microbiol 67:2723–2544
66. Smalla K, Wieland G, Buchner A, Zock A, Parzy J, Kaiser S, Roskot N, Heuer H, Berg G (2001) Bulk and rhizosphere soil bacterial communities studied by denaturing gradient gel electrophoresis: plant-dependent enrichment and seasonal shifts revealed. Appl Environ Microbiol 67:4742–4559
67. Smoot JC, Findlay RH (2001) Spatial and seasonal variation in a reservoir sedimentary microbial community as determined by phospholipid analysis. Microb Ecol 42:350–358
68. Stanford JA, Ward JV (1993) An ecosystem perspective of alluvial rivers: connectivity and the hyporheic corridor. J N Am Benthol Soc 12:48–60
69. Suzuki M, Giovannoni S (1996) Bias caused by template annealing in the amplification of mixtures of 16S rRNA genes by PCR. Appl Environ Microbiol 62:625–630
70. Takeda M, Koizumi J, Yabe K, Adachi K (1998) Thermostable poly(3-hydroxybutyrate) depolymerase of a thermophilic strain of *Leptothrix* sp. isolated from hot spring. J Ferment Bioeng 85:375–380
71. Van Hannen E, Mooij W, Van Agterveld M, Gons H, Laanbroek H (1999) Detritus-dependent development of the microbial community in an experimental system: qualitative analysis by denaturing gradient gel electrophoresis. Appl Environ Microbiol 65:2478–2484
72. Van Hannen EJ, Veninga M, Bloem J, Gons HJ, Laansbroek HJ (1999) Genetic changes in the bacterial community structure associated with protistan grazers. Arch Hydrobiol 145:25–38
73. Van Hannen EJ, Zwart G, Van Agterveld MP, Gons HJ, Ebert J, Laanbroek HJ (1999) Changes in bacterial and eukaryotic community structure after mass lysis of filamentous Cyanobacteria associated with viruses. Appl Environ Microbiol 65:795–801
74. Vaque D, Pace M, Findlay S, Lints D (1992) Fate of bacterial production in a heterotrophic ecosystem: grazing by protists

and metazoans in the Hudson Estuary. Mar Ecol Prog Ser 89:155–163

75. Ward JV, Bretschko G, Brunke M, Danjelopol D, Gibert J, Gonser T, Hildrew AG (1998) The boundaries of river systems: the metazoan perspective. Freshwat Biol 40:531–569
76. Weinbauer MG, Hofle MG (1998) Significance of viral lysis and flagellate grazing as factors controlling bacterioplankton production in a eutrophic lake. Appl Environ Microbiol 64:431–438
77. Woessner WW (2000) Stream and fluvial plain ground water interaction: rescaling hydrogeological thought. Ground Wat 38:423–429
78. Yu Z, Mohn WW (1999) Killing two birds with one stone: simultaneous extraction of DNA and RNA from activated sludge biomass. Can J Microbiol 45:269–272
79. Zhou J, Xia B, Treves DS, Wu L-Y, Marsh TL, O'Neill RV, Palumbo AV, Tiedje JM (2002) Spatial and resource factors influencing high microbiol diversity in soil. Appl Environ Microbiol 68:326–334
80. Zuker M, Mathews DH, Turner DH (1999) Algorithms and thermodynamics for RNA secondary structure prediction: a practical guide. In: Barciszewski J, Clark BFC (Eds.) RNA Biochemistry and Biotechnology. Kluwer Academic Publishers, Dordrecht, The Netherlands